Baseline Requirements For Detecting Biosignatures with the HabEx and LUVOIR Mission Concepts

Ji Wang[a,*], **Dimitri Mawet**[a], **Renyu Hu**[b,c], **Garreth Ruane**[a], **Jacques-Robert Delorme**[a], **Nikita Klimovich**[a]

[a]Department of Astronomy, California Institute of Technology, Pasadena, CA 91125, USA
[b]Jet Propulsion Laboratory, California Institute of Technology, Pasadena, CA 91109, USA
[c]Division of Geological and Planetary Sciences, California Institute of Technology, Pasadena, CA 91125, USA

arXiv:1806.04324v1 [astro-ph.EP] 12 Jun 2018

Abstract. A milestone in understanding life in the universe is the detection of biosignature gases in the atmospheres of habitable exoplanets. Future mission concepts under study by the 2020 decadal survey, e.g., HabEx and LUVOIR, have the potential of achieving this goal. We investigate the baseline requirements for detecting four molecular species, H_2O, O_2, CH_4, and CO_2, assuming concentrations of these species equal to that of modern Earth. These molecules are highly relevant to habitability and life on Earth and other planets. Through numerical simulations, we find the minimum requirements of spectral resolution, starlight suppression, and exposure time for detecting biosignature and habitability marker gases. The results are highly dependent on cloud conditions. A low-cloud case is more favorable because of deeper and denser lines whereas a no-cloud case is the pessimistic case for its low albedo. The minimum exposure time for detecting a certain molecule species can vary by a large factor ($\sim$10) between the low-cloud case and the no-cloud case. For all cases, we provide baseline requirements for HabEx and LUVOIR. The impact of exo-zodiacal contamination and thermal background is also discussed and will be included in future studies.

Keywords: HabEx, LUVOIR, Biosignature, Life, High Dispersion Coronagraphy.

***Further author information:** e-mail: ji.wang@caltech.edu

1 Introduction

Thousands of exoplanets have been discovered to date and many more will be detected by future missions. The focus of exoplanet studies are shifting towards understanding the statistical properties of exoplanets as a population and detailed characterization for scientifically-compelling nearby systems. One of the primary goals of the latter is to study the chemical composition of exoplanet atmospheres and the implications for habitability and life.

Habitability requires a surface temperature that is suitable for life and the existence of liquid water (H_2O). Therefore, H_2O is a high priority species to identity with future telescopes. In addition, biosignature gases, such as oxygen (O_2) and methane (CH_4), are highly indicative of life when co-existing out of thermodynamic equilibrium.[1] Carbon dioxide (CO_2) is the most prominent

greenhouse gas and is a key species to identify in habitable exoplanets. The total concentration of CO_2 is expected to differ on a habitable planet based on its position in the habitable zone. A low CO_2 concentration is expected for planets near the inner edge of the habitable zone and a high CO_2 concentration is expected for planets near the outer edge.[2] However, a high concentration of CO_2, together with high stellar UV flux, may produce abiotic O_2.[3–6] In this case, quantifying CO_2, O_2, and other gases will help rule out false positive scenarios. Future missions to detect and characterize habitable planets will have the ability to identify biosignature gases. However, there are several outstanding technical challenges:

- **Bigger aperture** Aperture size of future space missions will be marginally adequate to identify certain biosignature gases. For example, as shown in this paper, it is extremely challenging to detect CH_4 in certain cases.

- **Cooler system** Despite much stronger biosignature signals in the near infrared, it is likely that future large aperture space missions (4m-6.5m HabEx and 8m-16m LUVOIR) will not have the capability to operate at wavelengths longer than 1.8 μm because of increasing thermal background from the telescope system. To operate beyond 1.8 μm and have reasonably low thermal background, complicated cooling systems would be required , which may drastically increase the cost of the mission.

- **Higher spectral resolution** Identifying biosignature gases requires spectroscopic analysis of light from exoplanets. Most proposed dispersing elements for space missions to date have relatively low spectral resolution, e.g., R $\sim$ 70 for WFIRST-IFS,[7] which does not take advantage of rich spectral lines of the molecules of interest.

- **Better performance of adaptive optics systems** Ground-based extremely large telescopes

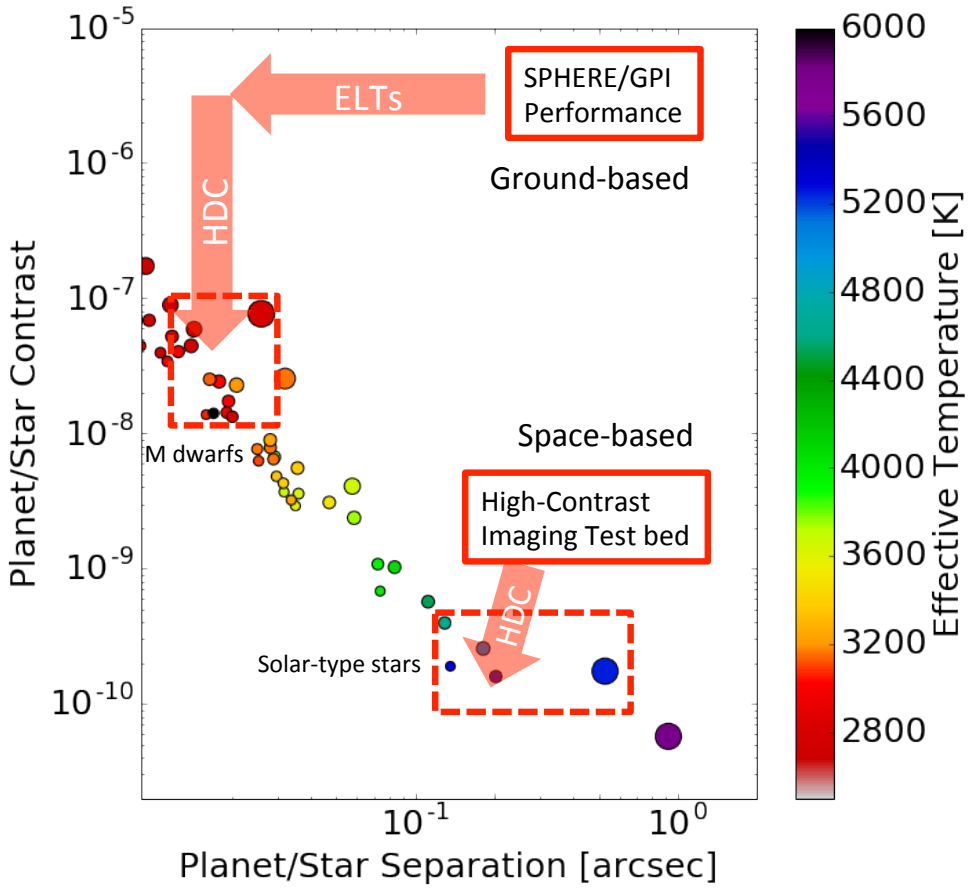


Fig 1 Planet-star contrast and angular separation for a hypothetical Earth-sized planet in the habitable zone around each star within 5 pc[2]. Each data point is colored by host star effective temperature and the size is scaled with distance. Red solid-lined boxes mark state-of-the-art performance for ground-based direct imaging instruments and test beds for future space-based missions. Red dashed-line boxes indicate the notional objectives for future ground-based missions (i.e., planets around M dwarfs) and for future space missions (i.e., planets around solar-type stars)

(ELTs) or Giant Segment Mirror Telescopes (GSMTs) will face severe challenges in breaking the current starlight suppression floor at $10^{-5}-10^{-6}$ level, which is set by adaptive optics system temporal bandwidth to correct for the Earth's atmospheric turbulence.

Fig. 1 summarizes the state-of-the-art performance of direct imaging instruments or testbeds (solid-lined boxes) and the requirements to detect a habitable planet (dashed-lined boxes). For both ground-based and space-based missions, there is a contrast gap between state-of-the-art performance and the planet-star contrast objective.

High dispersion coronagraphy (HDC) is a recent technical development that is designed to bridge the contrast gap.[8] HDC combines high contrast imaging (HCI), a single-mode fiber injection unit (FIU),[9] and high resolution spectroscopy (HRS) to filter out stellar light and extract the planet's signal. Specifically, HCI suppresses stellar light and spatially separates the planet from its host star. The FIU filters out stellar noise at the planet location since the electric field of a stellar speckles does not couple to the fundamental mode of a single-mode fiber, whereas up to $\sim 80\%$ of the planet light couples into the fiber. HRS further distinguishes planet signal from stellar signal by its unique spectral features such as absorption lines and radial velocity. Using this three-pronged starlight suppression, HDC can achieve the high sensitivity to study terrestrial planets in the habitable zone.

This paper focuses on the application of HDC on future space telescopes, e.g., HabEx and LUVOIR. The fundamental question we attempt to address here is whether these missions can detect four potential biosignature and habitability marker gases: O_2, CH_4, H_2O, and CO_2, and set mission requirements to achieve this goal. The four molecular species that are chosen have a relatively high concentration in the Earth's atmosphere and are significant signs of life. In addition, these species have been detected in earthshine and spacecraft observations of our own planet.[10] Detecting other biosignature gases , which have much lower concentrations, is expected to be far more challenging for exoplanets.

The paper is organized as follows. In §2, we briefly describe the four molecular species we investigate in this paper and the model we use to generate the spectra for our HDC simulations. In §3, we briefly describe our HDC simulation approach. More details can be found in previous work on HDC.[8,11] Results are given in §4 followed by summary and conclusion in §5.

2 MOLECULAR SPECIES OF INTEREST

2.1 Model Description

The spectra of Earth-like exoplanets are generated by an atmospheric chemistry and radiative transfer model.[3,12,13] We calculate the molecular abundance as a function of altitude, controlled by photochemical and disequilibrium chemistry processes.[3] The model atmosphere has been compared with terrestrial measurements in the mid-latitude and closely resembles the present-day Earth.[3] We calculate the disk-integrated reflected light spectra with an eighth-order Guassian integration and δ-2-stream approximation. We include the opacities of CO_2, O_2, H_2O, and CH_4 and calculate the planetary flux at a spectral resolution of $R = \lambda/\Delta\lambda = 500,000$, which is high enough to resolve individual spectral lines of the aforementioned species over $\lambda = 0.5$ - 5 μm.

It is well known that Earths disk-averaged spectrum cannot be reproduced by a single surface type or cloud deck.[14–16] Rather, it requires a combination of a cloud-free surface that is poorly reflective (i.e., the ocean), a highly reflective low cloud at ~ 4 km mimicking the cumulus clouds, and a high cloud at ~ 12 km mimicking the cirrus clouds.[14] We follow this treatment and assume the three types of surface or cloud. We assign equal weights to the three components to derive a reasonable account for an "Earth-like" planet. While the purpose is to reproduce Earth's spectrum, the resulting spectrum is generally consistent with the Earthshine experiments[14,15] as well as EPOXI measurements.[16]

2.2 Earth Spectrum By Molecule

We consider four molecular species in an Earth's atmosphere, CO_2, O_2, H_2O, and CH_4. Their spectra at different spectral resolutions are shown in Fig. 2. Observable line density and line depth decrease as spectral resolution decreases, making detecting certain molecules difficult at

low spectral resolutions. Conversely, planet signal is dispersed to more pixels at high spectral resolutions. In such a case, molecule detectability is generally limited by detector noise. Since there are a number of zero- or low-noise detectors that potentially allow us to overcome the detector noise limited case,[17] we assume noiseless detectors in the HDC simulations in this paper.

Planet reflection spectrum is highly dependent on cloud condition. Fig. 2 shows four cases: high-cloud, low-cloud, no-cloud, and the average of the three. The high-cloud case (orange) has the highest albedo, but line depth and density is the lowest, because the atmospheric column of absorbing gases above the cloud ($\sim$12 km) is the smallest. The effect is more notable for H_2O than for O_2, because the abundance of H_2O drops more than O_2 above the cloud. Consequently, The high-cloud case has the advantage of high reflection but the disadvantage of low spectral information content. In comparison, for the low-cloud case (red), lines are denser and deeper and the albedo is as high as the high-cloud case, so the low-cloud case represents the best case scenario for HDC observations. Lastly, the no-cloud case has the lowest albedo at < 0.1, because the cloud-free surface is poorly reflective.

Our averaged spectrum binned down to a low spectral resolution (e.g., $R = 300$) is generally consistent with Earthshine observations.[14] For example, the water absorption feature at 0.95 micron has an absorption depth of $\sim$50% according to Earthshine observation (see Fig. 6 in Ref. 14), consistent with our averaged spectrum (blue in Fig. 2). In comparison, the low-cloud case alone would have a greater continuum albedo and a deeper absorption.

We however recognize that the cloud coverage and heights will not be known *a priori* for any planets to be observed. In order to cover a large parameter space, we consider all three cases for different cloud conditions: the low-cloud case, the high-cloud case, and the no-cloud case. Results for the average-cloud case and any other cases should fall within the results of the three cases,

which will be discussed in subsequent sections.

Fig. 2 also emphasizes the need of going beyond 1 μm in order to detect biosignature gases. There are no strong lines of CH_4 and CO_2 below 1 μm. Detecting these two molecules is difficult at optical wavelengths. Even for molecules with strong lines below 1 μm, going beyond this wavelength would allow many more strong lines to be measured, thus increasing the detectability. We limit our HDC simulations below 1.8 μm, beyond which a cryogenic space mission would be required.

3 SIMULATIONS OF HDC OBSERVATIONS

3.1 Methodology

In this section, we briefly describe the procedure to simulate HDC observations and conduct data reduction. For more details in HDC simulations, please refer to two previous references.[8,11]

The planet and stellar spectra are convolved with a kernel that corresponds to a certain spectral resolution. The stellar signal is reduced by a factor that we refer to as the starlight suppression level. The starlight suppression includes the suppression from the coronagraph, wavefront control, and additional nulling boost provided by the use of a single-mode fiber.[9]

Poisson noise is added to account for photon noise. In addition, noises incurred in data reduction are included, e.g., errors associated with removing stellar light measured by additional fibers in speckle field. One particularly important noise source, speckle chromatic noise, is also taken into account. This noise arises from wavefront control at high starlight suppression levels and prevents us from detecting biosignature gases at low spectral resolutions.[8]

We briefly discuss here how the speckle chromatic noise confuses biosignature detection at low spectral resolutions and our strategy to remove the confusion. We refer readers to §6.4 in Ref.

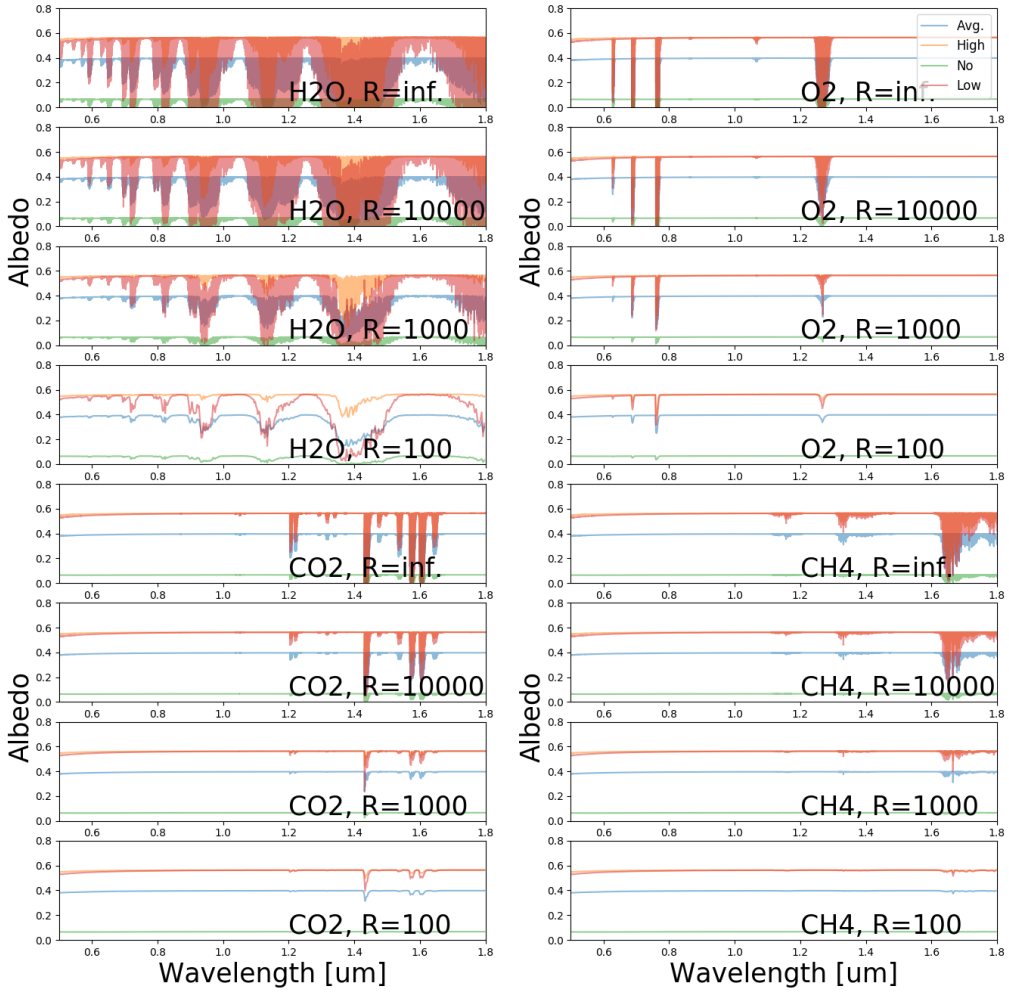


Fig 2 Albedo spectra for H_2O (top-left) O_2 (top-right), CO_2 (bottom-left), and CH_4 (bottom-right). Colors represent cases with different cloud conditions. Each panel has 4 rows to show the influence of spectral resolution on spectral features. Top row is for R>500,000 followed by R of 10000, 1000, and 100, respectively.

8 for more details. The speckle chromatic noise arises due to wavefront control at deep starlight suppression ($<\sim 10^{-7}$). Because wavefront control is normally optimized at a certain wavelength, starlight suppression is shallower at wavelengths that deviate from the optimal wavelength. As a result, speckle would have a parabolic spectral feature that sometimes mimics an absorption band of a molecule species. We name this speckle behavior at deep starlight suppression levels as the speckle chromatic noise. The speckle chromatic noise may be difficult to distinguish from absorption features of potential biosignatures, and this noise source therefore represents a potential false positive biosignature absorption signal.

At moderately high spectral resolutions, the speckle chromatic noise is no longer a concern because simulation has shown that the noise only has low-frequency spectral features. Therefore, our strategy of removing the speckle chromatic noise is straightforward. We apply a high-pass filter to those simulated observed spectra to remove spectral features with frequencies that correspond to R$<$100, where R is spectral resolution. In this procedure, both the speckle chromatic noise and the absorption features are removed. Our HDC simulations are no longer sensitive to spectral features with R$<$100. However, the simulations are free of the influence of the speckle chromatic noise. This makes direct comparison of our technique incompatible with other works at low resolutions (R$<$100) that do not employ a high-pass filter to mitigate the speckle chromatic noise.

The processed spectrum is then cross correlated with a template spectrum for the molecular species of interest and at the same spectral resolution as the observation. We note that the processed spectrum contains absorption features of all molecule species and have noise appropriately incorporated and thus represents a realistic case for HDC observations. The resulting cross correlation function (CCF) is used for biosignature detection and to access the relative abundance of different molecules that are present in planet's atmosphere. The key parameters used in HDC

simulations are given in Table 1.

Table 1 Inputs for HDC simulations for a Sun - Earth System

Telescope/Instrument		Star		Planet	
Telescope Aperture	4 m or 12 m	$T_{\rm eff}$	5800 K	Contrast	6×10^{-11}
End-to-End Throughput	10%	log(g)	4.5	Planet Radius	1.0 $R_\oplus$
Spectral Resolution	varied	$V \sin i$	2.7 km/s	$V \sin i$	0.5 km/s
Exposure Time	varied	Orbital Inclination	50 deg	Orbital Phase	0.25
Wavelength	0.5-1.8 μm	Radial Velocity	0.0 km/s	Radial Velocity	20.4 km/s
Detector Noise	0	Distance	5 pc	Semi-major Axis	1 AU

3.2 Detection Definition

Each HDC simulation results in a CCF. We repeat the HDC simulation 100 times for each combination of spectral resolution and starlight suppression level. We define significance of detection in the following way. The maximum CCF value within one spectral resolution element to the planet radial velocity is recorded for each run. After 100 runs, the distribution of maximum CCF values is obtained. We then calculate 16 and 84 percentiles, half of the difference between the two values corresponds to 1-σ of the distribution. This way of defining 1-σ is robust against outliers. The maximum CCF value divided by 1-σ gives detection significance. The median of detection significance values for 100 runs is recorded.

4 RESULTS

In this section, we summarize the requirements for detecting certain molecular species in terms of exposure time, spectral resolution, and starlight suppression level. Listed in order of decreasing difficulty, the molecules of interest are: CH_4, CO_2, O_2, and H_2O. The order of O_2, and H_2O may switch depending on spectral resolution and starlight suppression level. Results in this section will provide the baseline requirements for the three cases with different cloud conditions.

4.1 Requirements for HabEx

4.1.1 The No-Cloud Case

The no-cloud case has the lowest albedo (Fig. 2) and thus represents the worst case scenario. CH_4 cannot be detected even with an exposure time of 1600 hours (as shown in green contours in Fig. 3). Because of the low albedo, photon count is extremely low for the 4-m aperture of HabEx, there is on average 0.4 photon per pixel at the highest spectral resolution that we consider (R=51,200) for a 100-hour integration time. In addition, CH_4 lines are intrinsically rare and shallow at wavelengths shorter than 1.8 μm (see Fig. 2).

Detection of CO_2 is not possible even with an exposure time of 1600 hours because of the same reason as the CH_4 case for an albedo smaller than 0.1.

The minimum spectral resolution for O_2 detection is at R=700 and R=9,000 for 1600-hour and 400-hour exposure time and a starlight suppression level of 1×10^{-10}.

High spectral resolutions are necessary to relax the requirement for starlight suppression for O_2 detection. For example, at R=25600, starlight suppression can be relaxed to 2×10^{-10} and 1×10^{-9} for 400-hour and 1600-hour exposure time.

The minimum spectral resolution for H_2O detection is at R$\sim$240 and R$\sim$800 for 1600-hour and 400-hour exposure time and a starlight suppression level of 1×10^{-10}. Starlight suppression can be relaxed to a few times 10^{-8} at R=51,200 for an exposure time of 1600 hours. In a comparison to the O_2 case, higher spectral resolutions help more for the H_2O case because of the abundance of water lines across the whole wavelength range.

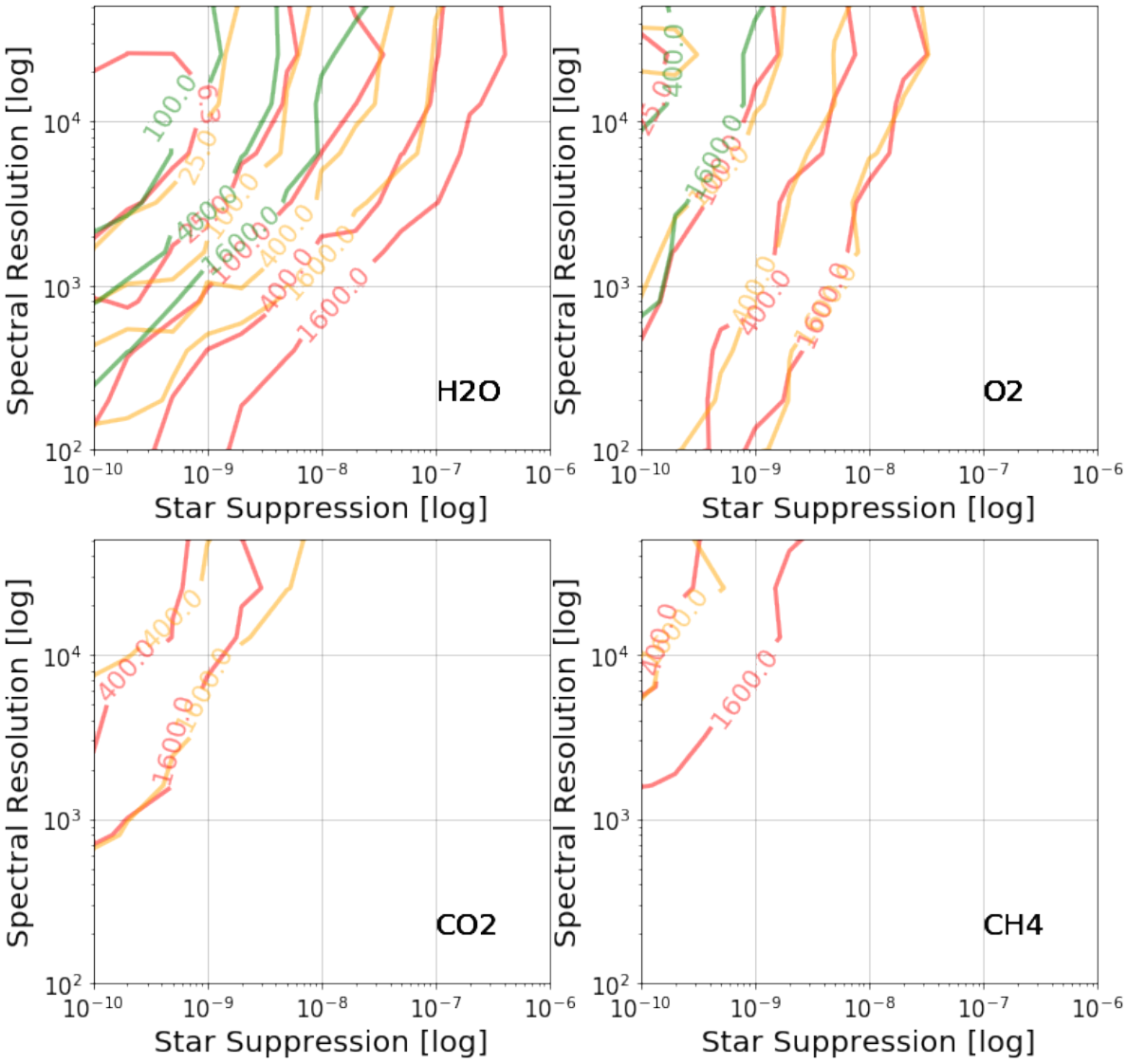


Fig 3 Exposure time contours (in hours) for 5-σ detection. Adjacent contours differ by a factor of 4 in exposure time. The simulation is for HabEx and assumes three cases with different cloud conditions: the no-cloud case (green), the high-cloud case (orange), and the low-cloud case (red).

4.1.2 The High-Cloud Case

The high-cloud case has a higher albedo but line depth is much shallower than the no-cloud case. However, the high albedo outweighs the shallow line depth, making it possible to detect all four gases.

The minimum spectral resolution for CH_4 detection is at R=5,000 for a 1600-hour exposure time and a starlight suppression level of 1×10^{-10}. It has been noted that a higher spectral resolution would help to increase detectability. However, even at R=256,000 and 1×10^{-10} starlight suppression, the minimum exposure time is 850 hours.

CO_2 can be detected for two exposure times that we consider, 400 hours and 1600 hours, for which the minimum spectral resolution is R=8,000 and R=700 at 1×10^{-10} starlight suppression, respectively. At R=51,200, the starlight suppression requirement can be relaxed to 5×10^{-9} and 1×10^{-9} for 1600-hour and 400-hour exposure times.

The requirement for O_2 detection is less stringent than CO_2 detection. Spectral resolution higher than 100 will suffice for starlight suppression levels deeper than 2×10^{-10} and 1×10^{-9} for exposure time of 400 and 1600 hours. The requirement for starlight suppression is further relaxed toward higher spectral resolutions with increasing exposure time (see orange contours in Fig. 3).

Because the speckle chromatic noise[8] is considered in our simulation, any low frequency spectral features are removed because of a high-pass filter that we have applied in the data reduction procedure. As a result, no molecules can be detected at a spectral resolution lower than R=100.

The minimum exposure time for H_2O detection is 12.7 hours at at R=25,600 and C=1×10^{-10}, where C denotes starlight suppression level. The requirement for starlight suppression can be relaxed by 3 orders of magnitude (compared to planet-star contrast at $\sim 10^{-10}$) at high spectral

resolutions (R>25,600) and for a long exposure time (i.e., 1600 hours). In this regime, the sensitivity boost of high dispersion coronagraphy is fully taken advantage because of sufficient photon flux and high spectral resolution.

4.1.3 The Low-Cloud Case

The main difference between the low-cloud case and the high-cloud case is line depth and density (see Fig. 2): spectral information is richer for the low-cloud case, which makes the case more amenable for spectroscopic observation. Red contours in Fig. 3 shows 5-σ detection significance contour. Notably, the 5-σ extends to lower spectral resolutions and shallower starlight suppression levels for H_2O and CH_4. Consequently, detection of these two molecule species is easier than the high-cloud case. This can be explained as follows: atmospheric column density for H_2O and CH_4 drops more than CO_2 and O_2, so a high cloud affects H_2O and CH_4 detectability more than CO_2 and O_2.

For CH_4, minimum exposure time is 300 hours at R=51,200 and C=1×10^{-10}. For longer exposure times, the requirement for both spectral resolution and starlight suppression can be relaxed. For example, the minimum spectral resolution is at R=1,400 and R=5,000 at C=1×10^{-10} for exposure time of 1600 and 400 hours. At a spectral resolution of 51,200, starlight suppression can be relaxed to 3×10^{-10} and 2×10^{-9} for exposure time of 400 and 1600 hours.

Detection of CH_4 in different cloud conditions exemplifies the influence of planetary spectrum on detection. The variety of possible planetary spectra may be the major uncertainty in estimating the minimum requirements for future space missions in search for biosignatures. We show here the influence of cloud condition. There are other uncertainties that may affect the mission sensitivity to biosignatures, for instance, the time evolution of Earth atmosphere. CH_4 concentration was

much higher in Archean Earth atmosphere.[18] Therefore, it is much easier to search for CH_4 for an Archean Earth.

The minimum exposure time for CO_2 detection is 150 hours at at R=51,200 and C=1×10^{-10}. The minimum spectral resolutions are R=700 and R=2,200 for exposure time of 1600 and 400 hours at a starlight suppression level of 1×10^{-10}. At the highest spectral resolution we consider (R=51,200), the minimum starlight suppression requirements are 7×10^{-10} and 2×10^{-9} for exposure time of 400 and 1600 hours.

The requirement for O_2 detection is similar to that for the high-cloud case.

The minimum exposure time for H_2O detection is 5 hours at at R=12,800 and C=1×10^{-10}. The requirement for starlight suppression can be relaxed by 3 orders of magnitude (compared to planet-star contrast at $\sim 10^{-10}$) at high spectral resolutions (R>25,600) and for long exposure times (>400 hours).

4.2 Requirements for LUVOIR

4.2.1 The No-Cloud Case

Green contours in Fig. 4 shows 5-σ detection contours at different exposure times for biosignatures for the LUVOIR no-cloud case. With a bigger aperture and thus higher photon flux, detection significance contours extend to lower spectral resolutions and shallower starlight suppression levels. Notably, the starlight suppression requirements are relaxed to $\sim 10^{-8}$ and 2×10^{-9} for H_2O and O_2 for an exposure time of 100 hours. We expect 100-hour as a reasonable exposure time for LUVOIR because it is a general purposed mission. CO_2 and CH_4 are not detectable given the 100-hour exposure time. The minimum exposure time for CO_2 and CH_4 detection is 183 hours and 354 hours at R=25,600 and C=1×10^{-10}. At the same combination of spectral resolution and

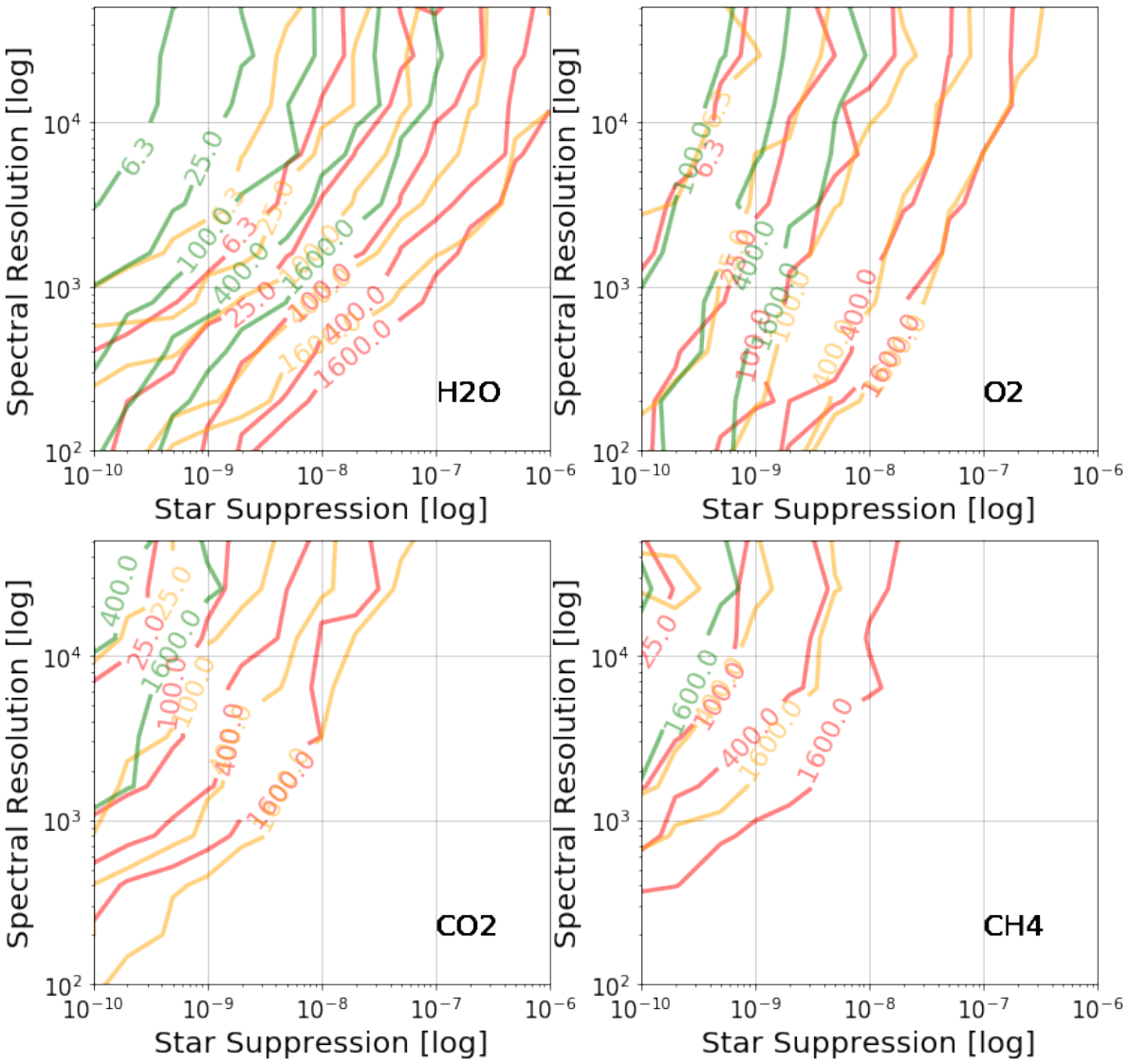


Fig 4 Exposure time contours (in hours) for 5-σ detection. Adjacent contours differ by a factor of 4 in exposure time. The simulation is for LUVOIR and assumes three cases with different cloud conditions: the no-cloud case (green), the high-cloud case (orange), and the low-cloud case (red).

starlight suppression level, the minimum exposure time for H_2O and O_2 detection is 5.0 and 25.0 hours.

4.2.2 The Low-Cloud Case

Red contours in Fig. 4 shows 5-σ detection contours at different exposure times for biosignatures for the LUVOIR low-cloud case. This represents the best case scenario for biosignature search

among all that we have considered in this paper. With an exposure time that shorter than 25 hours, all biosignatures can be detected at R=51,200 and C=1×10^{-10}. However, we must point out that the minimum exposure time is very sensitive to what type of cloud a planet may have. The minimum exposure time usually varies by a large factor. For example, the minimum exposure time for CH_4 detection differs by a factor of more than 10 between the no-cloud case (354 hours) and the low-cloud case (24 hours).

4.2.3 The High-Cloud Case

Orange contours in Fig. 4 shows 5-σ detection contours at different exposure times for biosignatures for the LUVOIR high-cloud case. For, H_2O and CH_4, the high-cloud contours recede towards higher spectral resolutions and deeper starlight suppression (i.e., upper-left corner of the parameter space in Fig. 4) when compared to the low-cloud case, indicating lower detectability of these two species in the high-cloud case. The high-cloud contours for O_2 are comparable between the low-cloud case and the high-cloud case, which is consistent with the HabEx result. The high-cloud contours for CO_2 indicate a higher detectability than the low-cloud case. However, we will show in §5.1 that the detectability is in fact comparable within uncertainties in exposure time calculation.

5 SUMMARY AND CONCLUSION

We study the detectability of four molecular species as biosignature or habitability indicators: CH_4, CO_2, O_2 and H_2O. We conduct HDC simulations to set the minimum requirements of exposure time, spectral resolution, and starlight suppression for the detection of these biosignatures. Major findings are summarized in Fig. 3, and Fig. 4. The implications are discussed in details in §4. The results provide a baseline for mission design in order to search for biosignature gases and study the

habitability of exoplanets.

The results of this paper are based on HDC simulations that focus on performance at high spectral resolutions. While the simulations are compatible with low resolution results, the cross-correlation may not be the best possible way to detect planets or molecules. A more straightforward way is to conduct a conventional ADI/SDI sequence, detecting the planet, obtaining a low-resolution spectrum, and inferring the molecular presence by measuring the absorption band depth. However, we provide two arguments for using the cross-correlation technique at low spectral resolutions. First, this ensures consistency in comparing performance over a broad range of spectral resolutions. Second, speckle chromatic noise may hinder molecule detection at low spectral resolutions with conventional method, the treatment in our HDC simulation ensures the effect of the speckle chromatic noise is properly modeled and removed.

5.1 Comparison to Previous Results

One major difference between this work and previous works on observing Earth-like planet using low resolution spectroscopy:[19] we consider speckle chromatic noise, which is a significant noise source at low spectral resolution (e.g., $R<100$).

Another difference is the definition of detection significance. In this work, we adopt the local variation of CCF peaks rather than the variation estimated from other parts of CCF. In previous works, the variation was estimated using the fluctuation of first quarter and/or the forth quarter of CCF. In principle, there should be no significant difference. However, using the local variation is more representative of CCF variation around CCF peak.

We compare our results to previous HDC simulations for HabEx and LUVOIR.[8,20] Using the same input planet spectrum, i.e., the average of the no-cloud case and the low-cloud case, we

compare the results for HabEx 400-hour exposure and LUVOIR 100-hour exposure (Fig. 5) to Fig. 20 and Fig. 15 in Ref. 8 to quantify the influence of difference definition of detection significance. We find that the contours in these two works track each other well with a maximum horizontal (i.e., starlight suppression level) difference by a factor of 2 at spectral resolution higher than R$\sim$2000. Part of the difference arises from statistical noise as it is evident that the contours are not smooth. The major difference between results in this paper and Fig. 20 and Fig. 15 in Ref. 8 is that we include speckle chromatic noise, which affects results at low spectral resolution significantly. Therefore, it is expected contours in Fig. 5 deviate from contours in Fig. 20 and Fig. 15 in Ref. 8 at lower spectral resolutions.

We also compare our results to Table 2 in Ref. 20 to check the consistency of exposure time calculation for different definitions of detection significance. We can check only one HabEx case for starlight suppression level shallower than 10^{-10} because HDC simulations in this work do not go deeper than 10^{-10}. At R=6,400 and C=5×10^{-10}, the exposure time for O_2 and H_2O detection is 162 hours and 404 hours. These values are comparable with values in Table 2 in Ref. 20 within a factor or 1.6. We also compare results for two LUVOIR cases (R=6400 and R=25600 at C=1×10^{-9}). For R=6400 and C=1×10^{-9}, the exposure time for CH_4, CO_2, O_2, and H_2O detection is $>$1600 hours, 406.2 hours, 72.1 hours, and 25.5 hours. Except for CH_4, exposure times for all other species are within a factor of 1.4 when compared to values in Table 2 in in Ref. 20. For CH_4, we have a lower limit for exposure time because our simulation stops at 1600 hours. For R=25,600 and C=1×10^{-9}, the exposure time for CO_2, O_2, and H_2O detection is 196.0 hours, 39.0 hours, and 18.0 hours. These values are also within a factor of 2 to values in Ref. 20.

Given the comparison with previous works, we conclude that the uncertainty of exposure time due to definition of detection significance and Poisson statistical noise is at most a factor of 2.

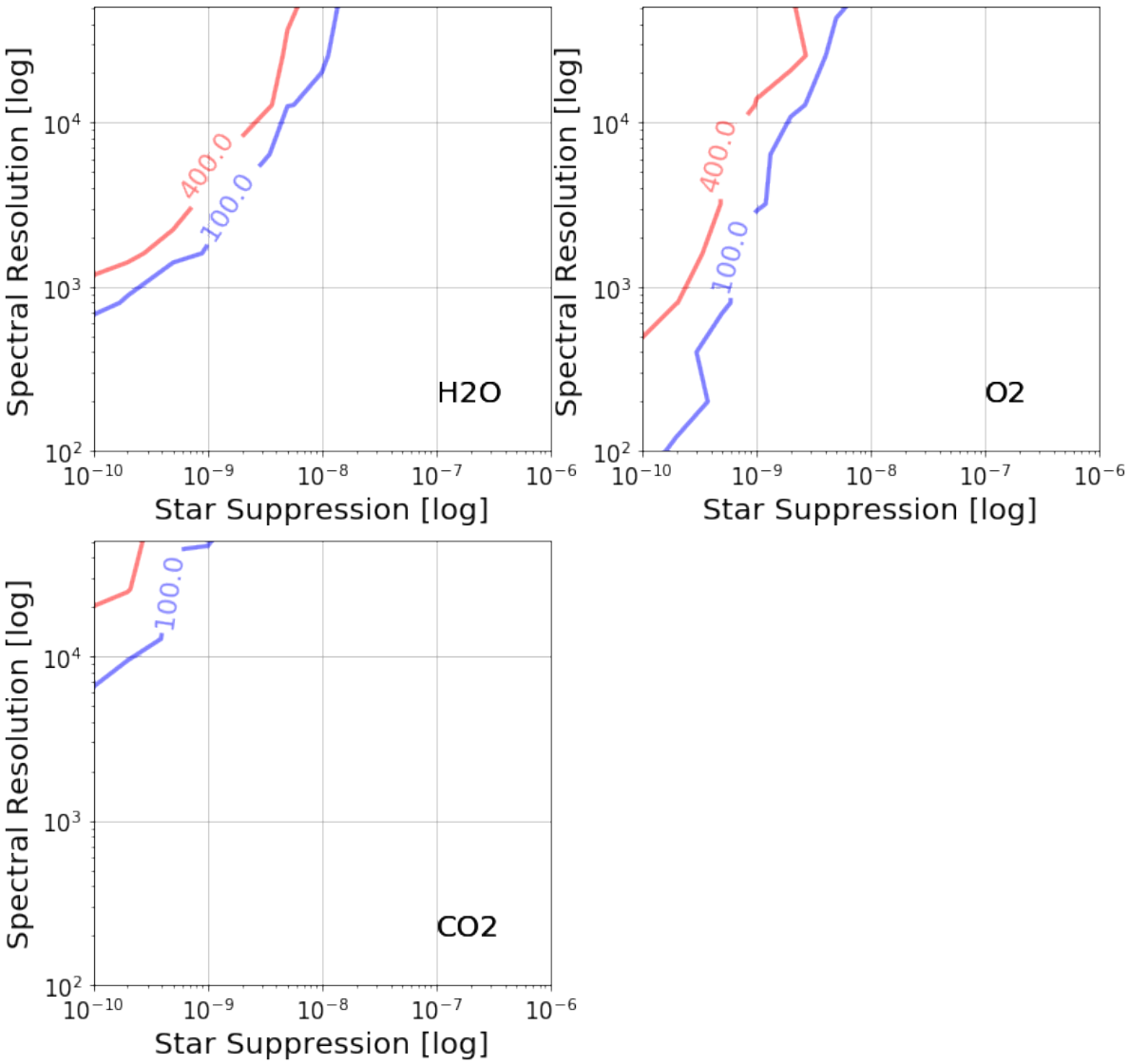


Fig 5 Exposure time contours (in hours) for 5-σ detection. Blue contours are for LUVOIR and red contours are for HabEx.

This uncertainty is smaller than the uncertainty due to cloud condition, which can change exposure time by a factor of ~ 10 between the low-cloud case and the no-cloud case. To account for the uncertainty of different definition of detection significance, we advise readers to use a error bar of 0.3 dex (i.e., a factor of 2) when using the minimum exposure time estimated in this paper for a given case of cloud condition.

For the speckle chromatic noise, we use a high-pass filter to remove speckle chromatic noise. As a result, low-frequency spectral features are also removed. This results in a much longer exposure time at low spectral resolution to reach a certain detection significance. For example, the exposure time is 80 hours for R=100 and C=1×10^{-10} for O_2 detection. In comparison, Ref. 19 estimated the exposure time is 200 hours for R=70 and C=1×10^{-10}. The difference can be explained as follows. First, the distance of the planet in their calculation was 10 pc. Factoring the difference would reduce the exposure time from 200 hours to 50 hours. Second, our error bar is 0.3 dex, so the actual exposure time can vary from 40 to 160 hours depending on the definition of detection significance. Therefore, the two results are consistent within uncertainty.

5.2 Exo-Zodiacal Flux and Thermal Backgound

We consider in our HDC simulation only starlight suppression levels that expected to be achieved by a coronagraphic system. However, the flux from exo-zodiacal dust may set a floor for the achievable starlight suppression level. This floor is estimated at a few times the planet-star contrast for a 4-m aperture, i.e., $\sim 10^{-10}$.[21,22] LUVOIR designs are less prone to exo-zodiacal flux because of a smaller point spread function and thus smaller contamination area. This is a result of the larger aperture of LUVOIR.

Another noise source that is not accounted for in our HDC simulation is the thermal background

emission from the telescope and instrument. This is not a typical concern at optical wavelengths. However, thermal background quickly becomes a severe issue at longer wavelengths. It is possible to consider a cryogenic system that cools the instrument to minimize thermal background and allows the instrument to operate at longer wavelengths. For example, mission designs exist that cool the system to 130 K without active cryogenic cooling: Euclid uses a passive cooling radiator system to cool the system to 130 K.[23] To be more realistic, we will incorporate both exo-zodiacal light emission and thermal noise in future versions of HDC simulation packages.

Acknowledgments

We would like to thank Rowan Swain for proofreading the manuscript. We thank anonymous referees for their comments and suggestions that greatly improve the paper.

References

1 D. J. Des Marais, M. O. Harwit, K. W. Jucks, *et al.*, "Remote Sensing of Planetary Properties and Biosignatures on Extrasolar Terrestrial Planets," *Astrobiology* **2**, 153–181 (2002).

2 R. K. Kopparapu, R. Ramirez, J. F. Kasting, *et al.*, "Habitable Zones around Main-sequence Stars: New Estimates," *ApJ* **765**, 131 (2013).

3 R. Hu, S. Seager, and W. Bains, "Photochemistry in Terrestrial Exoplanet Atmospheres. I. Photochemistry Model and Benchmark Cases," *ApJ* **761**, 166 (2012).

4 S. D. Domagal-Goldman, A. Segura, M. W. Claire, *et al.*, "Abiotic Ozone and Oxygen in Atmospheres Similar to Prebiotic Earth," *ApJ* **792**, 90 (2014).

5 F. Tian, K. France, J. L. Linsky, *et al.*, "High stellar FUV/NUV ratio and oxygen contents in

the atmospheres of potentially habitable planets," *Earth and Planetary Science Letters* **385**, 22–27 (2014).

6 C. E. Harman, E. W. Schwieterman, J. C. Schottelkotte, *et al.*, "Abiotic O_2 Levels on Planets around F, G, K, and M Stars: Possible False Positives for Life?," *ApJ* **812**, 137 (2015).

7 M. W. McElwain, A. M. Mandell, Q. Gong, *et al.*, "PISCES: an integral field spectrograph technology demonstration for the WFIRST coronagraph," in *Space Telescopes and Instrumentation 2016: Optical, Infrared, and Millimeter Wave*, *SPIE* **9904**, 99041A (2016).

8 J. Wang, D. Mawet, G. Ruane, *et al.*, "Observing Exoplanets with High Dispersion Coronagraphy. I. The Scientific Potential of Current and Next-generation Large Ground and Space Telescopes," *AJ* **153**, 183 (2017).

9 D. Mawet, G. Ruane, W. Xuan, *et al.*, "Observing Exoplanets with High-dispersion Coronagraphy. II. Demonstration of an Active Single-mode Fiber Injection Unit," *ApJ* **838**, 92 (2017).

10 S. Seager, W. Bains, and J. J. Petkowski, "Toward a List of Molecules as Potential Biosignature Gases for the Search for Life on Exoplanets and Applications to Terrestrial Biochemistry," *Astrobiology* **16**, 465–485 (2016).

11 J. Wang, D. Mawet, R. Hu, *et al.*, "High-contrast imaging and high-resolution spectroscopy observation of exoplanets," in *Modeling, Systems Engineering, and Project Management for Astronomy VI*, *SPIE* **9911**, 99112T (2016).

12 R. Hu, S. Seager, and W. Bains, "Photochemistry in Terrestrial Exoplanet Atmospheres. II. H_2S and SO_2 Photochemistry in Anoxic Atmospheres," *ApJ* **769**, 6 (2013).

13 R. Hu and S. Seager, "Photochemistry in Terrestrial Exoplanet Atmospheres. III. Photochemistry and Thermochemistry in Thick Atmospheres on Super Earths and Mini Neptunes," *ApJ* **784**, 63 (2014).

14 M. C. Turnbull, W. A. Traub, K. W. Jucks, *et al.*, "Spectrum of a Habitable World: Earthshine in the Near-Infrared," *ApJ* **644**, 551–559 (2006).

15 G. Tinetti, V. S. Meadows, D. Crisp, *et al.*, "Detectability of planetary characteristics in disk-averaged spectra. i: The earth model," *Astrobiology* **6**(1), 34–47 (2006).

16 T. D. Robinson, V. S. Meadows, D. Crisp, *et al.*, "Earth as an extrasolar planet: Earth model validation using epoxi earth observations," *Astrobiology* **11**(5), 393–408 (2011).

17 B. J. Rauscher, E. R. Canavan, S. H. Moseley, *et al.*, "Detectors and cooling technology for direct spectroscopic biosignature characterization," *Journal of Astronomical Telescopes, Instruments, and Systems* **2**, 041212 (2016).

18 S. Rugheimer and L. Kaltenegger, "Spectra of Earth-like Planets Through Geological Evolution Around FGKM Stars," *ArXiv e-prints* **000** (2017).

19 T. D. Robinson, K. R. Stapelfeldt, and M. S. Marley, "Characterizing Rocky and Gaseous Exoplanets with 2 m Class Space-based Coronagraphs," *PASP* **128**, 025003 (2016).

20 G. R. J.-R. D. N. K. R. H. Ji Wang, Dimitri Mawet, "Baseline requirements for detecting biosignatures with the habex and luvoir mission concepts," *Proc.SPIE* **10400**(9), 10400 (2017).

21 A. Roberge, C. H. Chen, R. Millan-Gabet, *et al.*, "The Exozodiacal Dust Problem for Direct Observations of Exo-Earths," *PASP* **124**, 799 (2012).

22 C. C. Stark, A. Roberge, A. Mandell, *et al.*, "Maximizing the ExoEarth Candidate Yield from a Future Direct Imaging Mission," *ApJ* **795**, 122 (2014).

23 G. D. Racca, R. Laureijs, L. Stagnaro, *et al.*, "The Euclid mission design," in *Space Telescopes and Instrumentation 2016: Optical, Infrared, and Millimeter Wave*, *SPIE* **9904**, 99040O (2016).

List of Figures

1 Planet-star contrast and angular separation for a hypothetical Earth-sized planet in the habitable zone around each star within 5 pc

2 Albedo spectra

3 Exposure time contours (in hours) for 5-σ detection

4 Exposure time contours (in hours) for 5-σ detection

5 Comparison to previous results

List of Tables

1 Inputs for HDC simulations for a Sun - Earth System